Role of Pressure Gradient on Intrinsic Toroidal Rotation in Tokamak Plasmas

M. Yoshida, Y. Kamada, H. Takenaga, Y. Sakamoto, H. Urano, N. Oyama, G. Matsunaga, and the JT-60 Team

Japan Atomic Energy Agency, Naka, Ibaraki-ken, 311-0193, Japan

(Received 3 May 2007; published 11 March 2008)

The toroidal plasma rotation generated by the external momentum input and by the plasma itself (intrinsic rotation) has been separated through a novel momentum transport analysis in the JT-60U tokamak device. The toroidal rotation, which is not determined by the momentum transport coefficients and the external momentum input, has been observed. It is found that this intrinsic rotation is locally determined by the local pressure gradient and increases with increasing pressure gradient. This trend is almost the same for various plasmas: low and high confinement mode, co and counterrotating plasmas.

DOI: 10.1103/PhysRevLett.100.105002 PACS numbers: 52.25.Fi, 52.30.−q, 52.55.Fa

Intrinsic toroidal plasma rotations generated by the plasma itself have recently become the subject of intense investigation in magnetically confined tokamak plasma research, since such an intrinsic rotation could dominate the total plasma rotation in future devices where the external momentum input from the auxiliary heating is expected to be small [1]. It is now widely recognized that the toroidal rotation velocity (V_t) and its radial shear play essential roles in determining magnetohydrodynamic stability at a high plasma pressure [2], and in the suppression of turbulence leading to enhanced confinement, such as the transport barrier formation [3]. Therefore, the critical importance of understanding the physical mechanisms determining the V_t profile including the intrinsic rotation, and controlling V_t profile has been increasingly recognized. The worldwide progress in understanding the physics of momentum transport and rotation has been made experimentally [4–8] and theoretically [9,10]. As for the elements determining the V_t, characteristics of momentum transport which consists of diffusive (the momentum diffusivity, χ_ϕ) and nondiffusive (the convection velocity, $V_{\rm conv}$) terms [8,11], the external momentum input and the intrinsic rotation [4–7] have been reported individually. However, the understanding of rotation mechanisms with integrating all of the terms (χ_ϕ, $V_{\rm conv}$, the external momentum input, and the intrinsic rotation) remains an open issue despite its urgency towards the next step devices. This is due mainly to an experimental difficulty in evaluating χ_ϕ, $V_{\rm conv}$ and the intrinsic rotation separately. In order to address this issue, we have applied the perturbation techniques developed in our recent works [8,11], which enable us to evaluate χ_ϕ and $V_{\rm conv}$ separately with external momentum input. In this Letter, the mechanisms determining the V_t profile is investigated in the various plasmas, such as low confinement mode (L mode), high confinement mode (H mode), CO (in the direction to the plasma current, I_p), and CTR (in the opposite direction to I_p) rotating plasmas. The neural beam (NB) heating power scan is carried out in order to investigate the roles of plasma pressure on the intrinsic rotation. From this approach, we have separately evaluated the roles of external induced rotation and the intrinsic rotation on the measured V_t profiles, and found the general dependence of intrinsic rotation in various confinement modes for the first time.

Experiments were conducted in the JT-60U tokamak [12] where NBs of various injection geometries are installed. They consist of two CO-tangential (CO-NBs), two CTR-tangential (CTR-NBs), and seven near perpendicular (CO- and CTR-PERP) beams. Five of the PERP-NBs are almost on-axis deposition, and the other two are off-axis. The injection angle of tangential beams is 36° and that of PERP-NBs (including the diagnostic NB for V_t and the ion temperature, T_i) is 75° with respect to the magnetic axis. The deuterium beam acceleration energy is about 85 keV, and the injection power per unit is about 2 MW.

An example of the intrinsic rotation for a weak positive magnetic shear L mode plasma with an internal transport barrier (ITB) is illustrated in Fig. 1. The main parameters for this plasma are $I_p = 1.4$ MA, the toroidal magnetic field $B_T = 4$ T, the major radius $R = 3.2$ m, the plasma minor radius $a = 0.8$ m, the safety factor at 95% flux surface $q_{95} = 5.1$. In this plasma, the toroidal momentum source (torque) density, which is calculated by the orbit following Monte Carlo code, is slightly CO-directed.

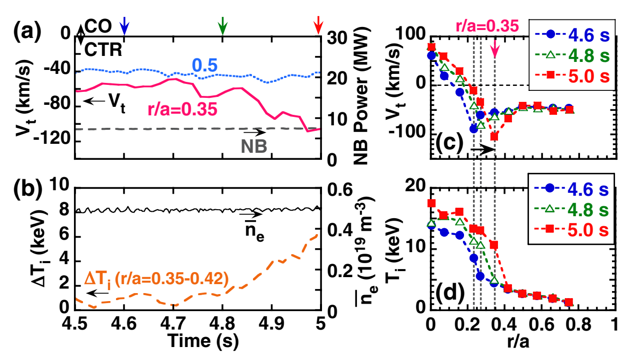

FIG. 1 (color online). Time traces of (a) toroidal rotation velocity (V_t) at $r/a = 0.35$ and 0.5, (b) difference in ion temperature (ΔT_i) between two positions ($r/a = 0.35$–0.42), and line averaged electron density ($\bar{n}_e$) for an L mode plasma with an internal transport barrier. Profiles of (c) V_t and (d) T_i at $t = 4.6$, 4.8, and 5.0 s.

Shown in Figs. 1(a) and 1(b) are the time traces of V_t and NB power, the difference in the T_i (ΔT_i) between two positions ($r/a = 0.35$ and 0.42) and the line averaged electron density ($\bar{n}_e$), respectively. Figures 1(c) and 1(d) illustrate the radial profiles of V_t and T_i at $t = 4.6$, 4.8 s, and 5.0 s, respectively. In this Letter, the positive and negative signs of V_t designate CO- and CTR-directed rotation, respectively. The V_t and T_i are measured from the Doppler shift and Doppler broadening of the 529.05 nm ($n = 8 - >7$) charge exchange emission from the interaction of fully stripped carbon impurity ions with NB, respectively. The diagnostic NB and the lines of sight of the diagnostic make an angle of ~90 degree. It is noted that the V_t at $r/a = 0.35$ clearly start to increase towards the CTR-direction in spite of constant CO-momentum input, when the ΔT_i starts to increase ($t \sim 4.8$ s) as shown in Figs. 1(a) and 1(b). The drop in V_t is observed in the region (dashed line) where a steep T_i gradient (gradT_i) appears at each time as shown in Figs. 1(c) and 1(d). The position of minimum V_t value moves from $r/a \sim 0.23$ to $r/a \sim 0.35$ accompanied with the shift of the steep gradT_i. On the other hand, the V_t profile does not change at all in the region $r/a > 0.4$ where T_i profile also does not change. The $\bar{n}_e$ remained almost constant as shown in Fig. 1(b). Therefore, the dominant factor in determining the pressure gradient is thought to be ΔT_i. From these results, the local pressure gradient seems to affect the local V_t.

In order to identify the contributions of the momentum transport and the intrinsic rotation to the V_t profile, one has to evaluate the momentum transport coefficients and V_t driven by external momentum input. We adopt the transient momentum transport analysis, which can separately determine χ_ϕ and $V_{\rm conv}$ [8,11], and reproduce the V_t profile using χ_ϕ, $V_{\rm conv}$ and external momentum source. By evaluating the difference between the reproduced rotation profile and the measured one, we evaluate the intrinsic rotation.

The analytical method for the determination of χ_ϕ and $V_{\rm conv}$ from source modulation experiments is described below. The toroidal momentum balance equation is written as

$$m_i \frac{\partial n_i V_t}{\partial t} = -\nabla \cdot \left(-m_i \chi_\phi \frac{\partial n_i V_t}{\partial r} + m_i V_{\rm conv} n_i V_t \right) + S, \quad (1)$$

where m_i, n_i, and S are the ion mass, the ion density, and the toroidal momentum source [8,11]. In this Letter, ions are defined as a sum of the main (deuterium) and impurity (carbon) ions, assuming that the toroidal rotation velocity of the main ions is the same as that of the impurity ions, i.e., the measured V_t. We confirmed the rotation speed of the bulk plasma from the mode frequency of sawtooth precursor ($m/n = 1/1$), neoclassical terming mode ($m/n = 3/2$) and the MHD modes at ITB ($n = 1$ and $n = 3$). The mode frequencies agree with the carbon ion toroidal rotation frequency. From these results, it is appropriate that the V_t of deuterium is assumed to be that of carbon. The effective charge number Z_{eff} was measured using visible bremsstrahlung, and its profile was assumed spatially uniform so that these values were capable of reproducing the measured neutron emission. When the modulated velocity part ($n_i^c \tilde{V}_t$) is much larger than the modulated density part ($\tilde{n}_i V_t^c$), the modulated $n_i V_t$ is expressed as follows [8] (the validity of this assumption in this experiment is shown later),

$$n_i^c \tilde{V}_t = n_i^c(r) V_{t0}(r) \sin[\omega t - \phi(r)], \quad (2)$$

where n_i^c is the time invariant terms of n_i, V_{t0}, ω, and ϕ are the amplitude of the modulated part of V_t, the modulation frequency and the phase delay of $\tilde{V}_t$, respectively. From the perturbed component of Eqs. (1) and (2), the time-independent solutions of χ_ϕ and $V_{\rm conv}$ can be obtained. Moreover, the V_t can be calculated from the momentum transport Eq. (1) using χ_ϕ and $V_{\rm conv}$, the boundary condition and the external momentum source.

Transient transport of toroidal momentum is demonstrated in L and H mode plasmas by using modulated injection of PERP-NBs, which enhances CTR rotation by the fast ion losses due to the toroidal field ripple in the peripheral region of the plasma [11]. L and H mode plasmas are chosen in order to investigate the basic mechanism of intrinsic rotation and momentum transport. Off-axis PERP-NBs (i.e., no external momentum input from modulated NBs [8], the absorbed power $P_{\rm ABS} \sim 2$ MW) are injected with a square wave modulation at 2 Hz. An example of the source modulation experiment in the H mode is shown in Fig. 2. The main plasma parameters are $I_p = 1.2$ MA, $B_T = 2.8$ T, $R = 3.4$ m, $a = 0.9$ m, and $P_{\rm ABS} = 6.0$ MW. Figure 2(a) shows the waveforms of modulated V_t at $r/a = 0.84$ (solid squares) and 0.30 (solid circles), and the total NB power. Each trace is fitted to a sinusoidal function at the modulation frequency (solid lines). In this analysis, we treat the edge rotation oscillation ($r/a \sim 0.85$) as the origin of momentum transport. In the inner area $r/a < 0.85$, the dominant components of the waveforms are sinusoidal. Therefore, we adopt the sinusoidal function to investigate the momentum transport. The radial profiles of ϕ and V_{t0} are shown in Figs. 2(b) and 2(c), respectively. The phase delay is taken from the start of NB injection. As shown in Fig. 2(b), the change in V_t to CTR-direction starts from the peripheral region and propagates to the core region because the driving source of CTR rotation is localized near the peripheral region [11]. The amplitude increases towards the core ($0.4 < r/a < 0.65$). This suggests the existence of an inward momentum flux. Figures 2(d) and 2(e) show χ_ϕ and $V_{\rm conv}$ as evaluated from ϕ and V_{t0} profiles in Figs. 2(b) and 2(c), respectively. As shown in Fig. 2(e), an inward convection velocity is observed in the region $0.4 < r/a < 0.65$. The modulated part of T_i is less than ±5%, and the phase delay of the modulated part of T_i is flat in the region $0.3 < r/a < 0.7$, unlike that of $\tilde{V}_t$. The value of the phase delay of ~80 degrees is

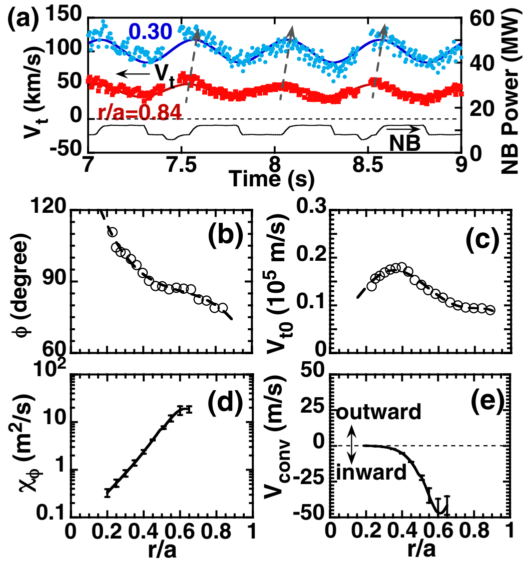

FIG. 2 (color online). (a) Response of V_t to modulated beams at $r/a = 0.84$ (solid square) and 0.30 (solid circles) in the H mode plasma. Waveform of NB power is also shown. Profiles of (b) phase delay (ϕ) and (c) modulated amplitude (V_{t0}) in Fig. 2(a). Profiles of (d) the toroidal momentum diffusivity (χ_ϕ) and (e) the convection velocity ($V_{\rm conv}$).

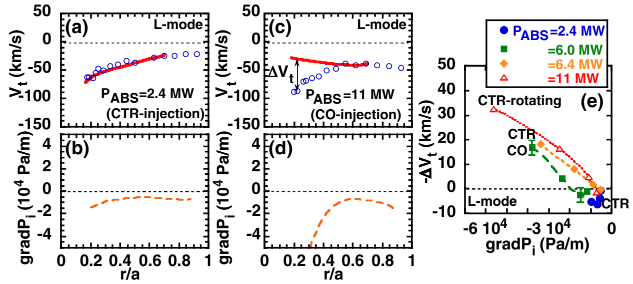

FIG. 3 (color online). (a) Profiles of the measured V_t (open circles) and the calculated one from the momentum equation with χ_ϕ and $V_{\rm conv}$ (solid line), (b) and pressure gradient (gradP_i) in the low $\beta_N = 0.39$ L mode plasma. (c) Profiles of the measured V_t and the calculated one, (d) and gradP_i in the higher $\beta_N = 1.07$ L mode plasma. (e) Difference between the measured V_t and the calculated one ($-\Delta V_t$) is plotted against the gradP_i in a heating power scan for L mode plasmas.

equal to ~50 ms (about a quarter of the slowing down time) from the start of NB injection. The T_i pedestal height is almost constant while the modulated NBs are injected. The amplitude of the modulated part of $\tilde{n}_e$, which is also fitted to a sinusoidal function, is about 1–2% of the time invariant value. If the n_i changes (is modulated) 1–2% with the same phase, the $n_i^c \tilde{V}_t$ is about 1 order of magnitude larger than the $\tilde{n}_i V_t^c$ in the region $0.2 < r/a < 0.7$. In the validity of this transient momentum transport analysis, we compare the measured V_t and the calculated one by the transient analysis.

A heating power scan is performed both in L mode ($I_p = 1.5$ MA, $B_T = 3.8$ T, $R \sim 3.4$ m, $a \sim 0.9$ m, $q_{95} = 4.2$, $\delta \sim 0.3$, and $\kappa \sim 1.3$–1.4) and in H mode plasmas ($I_p = 1.2$ MA, $B_T = 2.8$ T, $R \sim 3.4$ m, $a \sim 0.9$ m, $\delta \sim 0.33$, and $\kappa \sim 1.4$). For the L mode plasmas, $P_{\rm ABS}$ is varied over the range 2.4 MW $< P_{\rm ABS} <$ 11 MW. For the H mode plasmas, two units of CO-tangential NBs are injected constantly, and the number of PERP-NB units is scanned from one to four units; i.e., the absorbed power varied over the range 4.8 MW $< P_{\rm ABS} <$ 10 MW. The normalized beta (β_N) varies from 1.1 to 1.8. Here, β_N is defined as $\beta_N = (\beta_t a B_{t0})/I_p$, where β_t is the ratio of the plasma pressure to the pressure of B_T and B_{t0} is the toroidal magnetic field at the plasma center.

Figure 3(a) shows the radial profile of the measured V_t (open circles) in the case of a low $\beta_N (\beta_N = 0.39)$ L mode plasma where the ion thermal pressure gradient (gradP_i) is small as shown in Fig. 3(b) (dotted line). In this plasma, a half unit of CTR-NB and one unit of PERP-NB are injected. The solid line in Fig. 3(a) shows the calculated V_t from the momentum transport Eq. (1) using χ_ϕ and $V_{\rm conv}$ with the boundary condition (setting the measured V_t equal to the calculated one at $r/a \sim 0.65$) [11]. As shown in Fig. 3(a), the measured V_t agrees with the calculated one in the region $0.15 < r/a < 0.65$ in low β_N plasmas [8,11]. Shown in Figs. 3(c) and 3(d) are the data in the case with a higher $\beta_N (\beta_N = 1.07)$ L mode plasma where the heating power increases to 11 MW. Although the measured V_t agrees with the calculation in the region $0.45 < r/a < 0.65$, the measured V_t deviates from the calculated one in the CTR-direction in the core region $0.2 < r/a < 0.45$. In the plasma regime treated in this Letter, the difference between the deuterium V_t and the carbon V_t predicted from the neoclassical theory [13] is negligibly small. For example, in the L mode plasma shown in Fig. 3(c), the difference between the deuterium V_t and the carbon V_t is about 3–7 km/s in the region $r/a = 0.45$–0.2. This value is much smaller than both the target V_t of -50–-90 km/s and the difference between the measured V_t and the calculated one. These results mean that the measured V_t cannot be explained with the momentum transport model including momentum transport coefficients, the boundary condition of V_t, and the external momentum input by NBs. In higher β_N plasma, the large gradP_i is observed in the core region ($0.2 < r/a < 0.45$) as shown in Fig. 3(d). In order to investigate the relation between the increase of CTR rotation and the gradP_i, the difference between the measured V_t and the calculated one, i.e., $\Delta V_t = V_t(measurement) - V_t(calculation) = intrinsic\ rotation$ in the region $0.3 < r/a < 0.6$ is plotted against the gradP_i in the heating power scan in Fig. 3(e). The symbols denote ΔV_t at $r/a = 0.3$, 0.4, 0.5, and 0.6. In these L mode plasmas, the larger values of gradP_i are obtained in the core region. As shown in Fig. 3(e), ΔV_t grows with increasing gradP_i in all cases. This tendency is almost the same, even the direction of the V_t is different (CO- and CTR-rotating plasmas), over a wide range of χ_ϕ which varies by about 1 order of magnitude radially

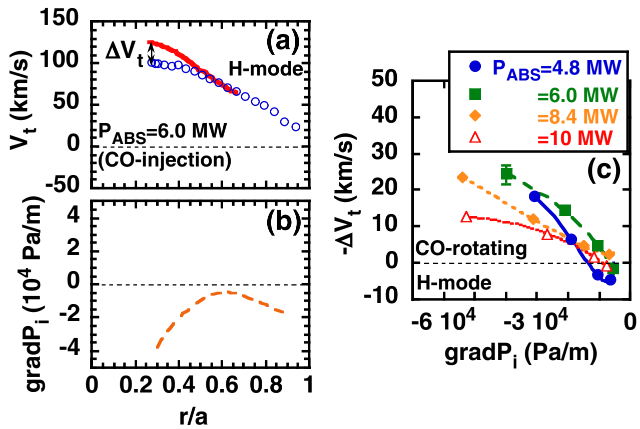

FIG. 4 (color online). (a) Profiles of the measured V_t (open circles) and the calculated one (solid line), (b) and gradP_i in the H mode plasma ($\beta_N = 1.29$). (c) Dependence of $-\Delta V_t$ on gradP_i in a heating power scan for H mode plasmas.

($\chi_\phi \sim$ 1–30 m^2/s) and by about a factor of 3 ($\chi_\phi \sim$ 1–3 m^2/s) (in the heating power scan) at fixed radius ($r/a \sim 0.4$). These results indicate gradP_i affects the intrinsic rotation even in L mode plasmas, and the local gradP_i affects the local value of the intrinsic rotation.

Figure 4(a) illustrates the measured V_t profile (open circles) in the H mode plasma with $P_{\rm ABS} = 6.0$ MW (same discharge shown in Fig. 2) and the V_t profile calculated from Eq. (1) (solid line) using transport coefficients in Figs. 2(d) and 2(e). As shown in Fig. 4(a), the measured V_t agrees with the calculation in the region $0.45 < r/a < 0.65$; however, in the core region $0.2 < r/a < 0.45$, the measured V_t deviates from the calculated one in the CTR-direction, and the large pressure gradients is observed in the core region ($0.2 < r/a < 0.45$) as shown in Fig. 4(b) similar to the results found in the L mode plasma [Figs. 3(c) and 3(d)]. Figure 4(c) shows the dependence of $-\Delta V_t$ on the gradP_i in the region $0.3 < r/a < 0.6$ in the heating power scan in H mode. Here again, the symbols denote ΔV_t at $r/a = 0.3$, 0.4, 0.5, and 0.6. The ΔV_t grows with increasing gradP_i in H mode plasmas as well as L mode plasmas [Fig. 3(e)]. The good correlation between the local intrinsic rotation velocity and the local gradP_i indicates that the gradP_i appears to cause the value of the local intrinsic rotation velocity.

The direction of the intrinsic rotation is the same as that of the toroidal component of the $\mathbf{E}_{{\rm grad}P} \times \mathbf{B}$ velocity ($V_{{\rm Egrad}P\times Bp}$) and is the opposite to that of the toroidal component of the diamagnetic drift velocity (V_{Di}). Here, $E_{{\rm grad}P}$ is the contribution to the radial electric field from only the carbon pressure gradient (i.e., $\nabla p_c/Zen_c$, where p_c is the carbon pressure, Ze is the electronic charge of the C^{6+} ions, n_c is the carbon density) and B_p is the poloidal magnetic field. However, the values of $V_{{\rm Egrad}P\times Bp}$ and V_{Di} are about -0.1 and 0.1 km/s, respectively, and about 2 orders of magnitude smaller than that of the intrinsic rotation at $r/a = 0.3$ in the H mode plasma with $P_{\rm ABS} =$ 6 MW shown in Fig. 4. With respect to Fig. 1, the general trend shown in Figs. 3 and 4 provides a possible explanation for the relation between V_t and ΔT_i, although the evaluation of χ_ϕ and $V_{\rm conv}$ is needed for more details. In addition to the pressure gradient, an investigation of the effects of other factors on the intrinsic rotation is an important issue in order to explain the variation of ΔV_t in Fig, 4(c). The present results may also be related to the theory [9], which suggests that a residual stress can drive the intrinsic rotation, and the stress is driven by the gradP_i/n_i shear.

In conclusion, we have identified the intrinsic rotation, which is not determined by the momentum transport coefficients and the external momentum input. A change of V_t towards the CTR-direction is clearly observed, when the ΔT_i starts to increase with constant momentum input (Fig. 1). In order to investigate the contribution of the intrinsic rotation to actual/measured V_t profiles, we separately evaluate the rotation, which is driven by the external momentum input and the plasma itself using the transient momentum transport analysis. A good correlation between the intrinsic rotation (ΔV_t) and the pressure gradient is found: the intrinsic rotation increases with increasing pressure gradient in various plasmas including L mode, H mode, CO-, and CTR-rotating plasmas (Figs. 3 and 4). The local pressure gradient plays the role in determining the local value of intrinsic rotation velocity. This means that the intrinsic rotation affected by gradP_i does not diffuse radially. These results imply that this trend is general and fundamental, and this trend shown in Figs. 3 and 4 provides a possible explanation for the behavior of V_t and T_i for the plasmas with ITB shown in Fig. 1. This study provides an important framework for integrating the effects of the diffusive and the nondiffusive terms of momentum transport, external momentum input, and intrinsic rotation.

[1] Special issue on Progress in the ITER Physics Basis [Nucl. Fusion **47**, S18 (2007)].
[2] H. Reimerdes *et al.*, Phys. Rev. Lett. **98**, 055001 (2007).
[3] Y. Sakamoto *et al.*, Nucl. Fusion **41**, 865 (2001).
[4] W. D. Lee *et al.*, Phys. Rev. Lett. **91**, 205003 (2003).
[5] J. E. Rice *et al.*, Nucl. Fusion **47**, 1618 (2007).
[6] A. Bortolon *et al.*, Phys. Rev. Lett. **97**, 235003 (2006).
[7] K. Ida *et al.*, J. Phys. Soc. Jpn. **67**, 4089 (1998).
[8] M. Yoshida *et al.*, Nucl. Fusion **47**, 856 (2007).
[9] O. D. Gurcan *et al.*, Phys. Plasmas **14**, 042306 (2007).
[10] B. Coppi, Nucl. Fusion **42**, 1 (2002).
[11] M. Yoshida *et al.*, Plasma Phys. Controlled Fusion **48**, 1673 (2006).
[12] S. Ide and (The JT-60 Team), Nucl. Fusion **45**, S48 (2005).
[13] Y. B. Kim, P. H. Diamond, and R. J. Groebner, Phys. Fluids B **3**, 2050 (1991).